Pergamon

Int. J. Solids Structures Vol. 34, No. 12, pp. 1463–1478, 1997

0020–7683/97 $17.00 + .00

PII: S0020–7683(96)00086–8

TRANSIENT THREE-DIMENSIONAL RAYLEIGH AND STONELEY SIGNAL EFFECTS IN THERMOELASTIC SOLIDS

L. M. BROCK
Mechanical Engineering, University of Kentucky, Lexington, Kentucky 40506, U.S.A.

(*Received* 15 *September* 1995; *in revised form* 9 *May* 1996)

Abstract—A transient 3D study of surface (Rayleigh) and interface (Stoneley) signals in fully-coupled thermolastic solids begins by obtaining analytical expressions for the zeroes of the corresponding Rayleigh/Stoneley functions that arise in the integral transforms of the solutions. The expressions locate the zeroes as functions of the temporal transform variable in a complex plane defined by a scalar resultant of spatial transform variables.

Expressions for the change in surface temperature caused by the Rayleigh signal are then derived for cases of normal traction surface loading. By using long-time asymptotic results, the expressions can be obtained analytically, and they show that Rayleigh/Stoneley signal-induced thermal effects can be important.

The long-time asymptotic results also show that Rayleigh/Stoneley zeroes reduce to the thermally-modified inverses of the classical (non-thermal) Rayleigh/Stoneley wave speeds. This result agrees with 2D predictions that can be made on the basis of low-frequency asymptotic harmonic wave studies. The long-time results are not restrictive, because time is scaled by a small, i.e., $O(10^{-4})\mu$m, thermoelastic characteristic length. © 1997 Elsevier Science Ltd. All rights reserved.

INTRODUCTION

Surface (Lamb, 1904) and interface (Stoneley, 1924) waves are important phenomena in elastic materials. Such waves may dominate surface/interface response (Achenbach, 1973; Miklowitz, 1978) and their speeds may characterize limiting propagation rates for cracks (Freund, 1990; Liu *et al.*, 1995). Moreover, surface wave arrivals at crack edges may cause an instantaneous transition of the stress intensity factor to a static value (Freund, 1974; Brock, 1982a).

Surface/interface phenomena can also occur for fully-coupled thermoelastic solids. They may be somewhat different because, unless the standard Fourier heat flow law is modified (Joseph and Preziosi, 1989) only one classical body wave—the rotational wave—occurs in an isotropic material. Nevertheless, signals analogous to Rayleigh (surface) waves have been studied in the frequency domain (Chadwick, 1960; Nowinski, 1978) and found for low frequencies to behave like classical Rayleigh waves traveling at modified speeds.

Recently (Brock, 1995), transient 2D studies were made of Rayleigh signals in a thermoelastic half-plane and Stoneley (interface) signals in two rigidly-joined thermoelastic half-planes. Particular attention was paid to the zeroes of the associated Rayleigh/Stoneley functions in the solution integral transform space, following the model of Cagniard's (1962) work on classical (non-thermal) Stoneley waves. No appeal to asymptotics was made, and analytic expressions for the zeroes in terms of the temporal transform variable were obtained. The zeroes were then examined for long-time behavior and found to reduce to the inverse of thermally-modified Rayleigh/Stoneley speeds, c.f. (Chadwick, 1960; Nowinski, 1978). The long-time results were, however, robust because time was scaled by an extremely small thermoelastic characteristic length.

The present study extends this work by first considering the 3D transient situation for fully-coupled thermoelastic half-spaces. Both mechanical and thermal surface/interface conditions are imposed. Then, the effects of surface/interface signal response are illustrated for Rayleigh signal examples in terms of the long-time surface temperature changes associated with the signals. The study begins in the next section with the 3D Rayleigh signal problem formulation.

RAYLEIGH SIGNAL PROBLEM: FORMULATION

Consider the half-space defined in terms of Cartesian coordinates $\mathbf{x} = (x, y, z)$ and corresponding basis vectors $(\mathbf{i}, \mathbf{j}, \mathbf{k})$ as the region $z > 0$. For time $t \leqslant 0$ the half-space is at rest at a uniform temperature $T_o(K)$. For $t > 0$ the half-space surface is subjected to normal and shear tractions and to a specified heat flux. The governing equations for a linearly thermoelastic, isotropic solid can, after Chadwick (1960), be written as

$$\nabla^2\mathbf{u} + \frac{1}{1-2\nu}\nabla\Delta - 2\frac{1+\nu}{1-2\nu}\kappa_o\nabla\omega - \frac{\rho}{\mu}\ddot{\mathbf{u}} = 0 \tag{1a}$$

$$k\nabla^2\omega - \rho c_h\dot{\omega} - 2\frac{1+\nu}{1-2\nu}\mu\kappa_o T_o\dot{\Delta} = 0 \tag{1b}$$

$$\frac{1}{\mu}\boldsymbol{\sigma} = \left(\frac{\nu}{1+\nu}\Delta - 2\frac{1+\nu}{1-2\nu}\kappa_o\omega\right)\mathbf{I} + \nabla\mathbf{u} + \mathbf{u}\nabla \tag{1c}$$

for $z > 0$, $t > 0$. Here $\mathbf{u}(\mathbf{x}, t) = (u_x, u_y, u_z)$ is the displacement vector, $\boldsymbol{\sigma}$ is the stress tensor, $\omega(\mathbf{x}, t)$ is the change in temperature from T_o, Δ is the dilatation and $(\cdot)$ denotes t-differentiation. The constants $(\mu, \nu, \rho, \kappa_o, k, c_h)$ are, respectively, the shear modulus, Poisson's ratio, mass density, coefficient of thermal expansion, conductivity and specific heat. For $z > 0$, $t \leqslant 0$ we have

$$\mathbf{u}, \omega \equiv 0 \tag{2}$$

while for $z = 0$, $t > 0$ the conditions

$$\boldsymbol{\sigma}\cdot\mathbf{k} = (\tau_x, \tau_y, \sigma), \quad \frac{\partial\omega}{\partial z} = F \tag{3a, b}$$

hold, where $(\tau_x, \tau_y, \sigma, F)$ are piecewise continuous functions of (ρ, t) and bounded in $\boldsymbol{\rho}$ for finite $t > 0$, where $\boldsymbol{\rho} = (x, y, 0)$. In addition, $(\mathbf{u}, \omega)$ are bounded in $\mathbf{x}$ for finite $t > 0$ and continuous in $(\mathbf{x}, t)$.

To solve the problem (1)–(5), the constants

$$v_r = \frac{1}{b} = \sqrt{\frac{\mu}{\rho}}, \quad v_d = \frac{1}{a} = mv_r, \quad m = \sqrt{2\frac{1-\nu}{1-2\nu}} \tag{4a}$$

$$h = \frac{kv_r}{\mu m c_h}, \quad \varepsilon = \frac{T_o}{c_h}\left(\frac{\kappa v_r}{m}\right)^2, \quad \kappa = \kappa_o(4-3m^2) < 0 \tag{4b}$$

are introduced, where (v_r, v_d) are the classical rotational and dilatational waves speeds, (b, a) are the corresponding slownesses, h is a thermoelastic characteristic length and ε is dimensionless. A classical dialational wave may not actually arise in the coupled thermoelastic solid, but both wave speeds and their dimensionless ratio m enter into the problem formulation. The length h is generally of order $O(10^{-4})\mu$m (Brock, 1992) while the so-called coupling constant ε is of order $O(10^{-2})$ (Chadwick, 1960). Substitution of (6) and (7) into (1)–(3) gives the more compact forms

$$\nabla^2\mathbf{u} + (m^2-1)\nabla\Delta + \kappa\nabla\omega - b^2\ddot{\mathbf{u}} = 0 \tag{5a}$$

$$\frac{h}{a}\nabla^2\omega - \dot{\omega} + \frac{m^2\varepsilon}{\kappa}\dot{\Delta} = 0 \tag{5b}$$

$$\frac{1}{\mu}\boldsymbol{\sigma} = [(m^2-2)\Delta + \kappa\omega]\mathbf{I} + \nabla\mathbf{u} + \mathbf{u}\nabla. \tag{5c}$$

The system (2)–(5) can be addressed by employing the unilateral (Sneddon, 1972) and bilateral (van der Pol and Bremmer, 1950) Laplace transforms

$$\hat{f}=\int_0^\infty f(t)\,\mathrm{e}^{-st}\,\mathrm{d}t,\quad f^*=\iint \hat{f}(\mathbf{x})\,\mathrm{e}^{-s(\mathbf{p}\cdot\boldsymbol{\rho})}\,\mathrm{d}x\,\mathrm{d}y \tag{6a, b}$$

$$\mathbf{p}=(p,q,0) \tag{6c}$$

over the temporal and spatial variables t and $\boldsymbol{\rho}$. In (6) s can be taken to be real and positive, while $\mathbf{p}$ is, in general, complex, and integration in (6b) is over the entire xy-plane. Application of (6a, b) to (5) gives in view of (2) the transform solution

$$\begin{bmatrix}\omega^*\\ su_x^*\\ su_y^*\\ su_z^*\end{bmatrix}=\begin{bmatrix}\lambda_+ & \lambda_- & 0 & 0\\ -p & -p & \beta & 0\\ -q & -q & 0 & \beta\\ \pm\alpha_+ & \pm\alpha_- & \pm p & \pm q\end{bmatrix}\begin{bmatrix}A_+\,\mathrm{e}^{-s\alpha_+|z|}\\ A_-\,\mathrm{e}^{-s\alpha_-|z|}\\ \frac{1}{\beta}B_x\,\mathrm{e}^{-s\beta|z|}\\ \frac{1}{\beta}B_y\,\mathrm{e}^{-s\beta|z|}\end{bmatrix} \tag{7a}$$

$$\begin{bmatrix}\sigma_{xy}^*\\ \sigma_{xz}^*\\ \sigma_{yz}^*\\ \sigma_x^*\\ \sigma_y^*\\ \sigma_z^*\end{bmatrix}=\mu\begin{bmatrix}-2pq & -2pq & q\beta & p\beta\\ \pm 2p\alpha_+ & \pm 2p\alpha_- & \mp T_q & \pm pq\\ \pm 2q\alpha_+ & \pm 2q\alpha_- & \pm pq & \mp T_p\\ T_{q+} & T_{q-} & 2p\beta & 0\\ T_{p+} & T_{p-} & 0 & 2q\beta\\ -T & -T & -2p\beta & -2q\beta\end{bmatrix}\begin{bmatrix}A_+\,\mathrm{e}^{-s\alpha_+|z|}\\ A_-\,\mathrm{e}^{-s\alpha_-|z|}\\ \frac{1}{\beta}B_x\,\mathrm{e}^{-s\beta|z|}\\ \frac{1}{\beta}B_y\,\mathrm{e}^{-s\beta|z|}\end{bmatrix} \tag{7b}$$

bounded for $z>0(+)$ and $z<0(-)$. Here $A_\pm$ and $\mathbf{B}=(B_x,B_y,0)$ are arbitrary functions of $(s,\mathbf{p})$ and

$$\alpha_\pm=\sqrt{b_\pm^2-r^2},\quad \beta=\sqrt{b^2-r^2},\quad T=b^2-2r^2,\quad T_\pm=2\alpha_\pm^2-b^2 \tag{8a}$$

$$T_p=T+p^2,\quad T_q=T+q^2,\quad T_{p\pm}=T_\pm+2p^2,\quad T_{q\pm}=T_\pm+2q^2 \tag{8b}$$

$$b_\pm=m_\pm a,\quad \kappa\lambda_\pm=b^2M_\pm \tag{8c}$$

$$M_\pm=m_\pm^2-1,\quad 2m_\pm=\sqrt{\left(1+\frac{1}{\sqrt{\tau}}\right)^2+\frac{\varepsilon}{\tau}}\pm\sqrt{\left(1-\frac{1}{\sqrt{\tau}}\right)^2+\frac{\varepsilon}{\tau}},\quad M_+M_-=-\frac{\varepsilon}{\tau} \tag{8d}$$

where

$$r=\sqrt{\mathbf{p}\cdot p}=\sqrt{p^2+q^2},\quad \tau=ahs \tag{9}$$

are dimensionless transform variables. Dependence on the scalar resultant r, not $\mathbf{p}$ itself, allow $(\alpha_\pm,\beta)$ to be viewed as functions in complex r-planes. Then, boundedness requires that $\mathrm{Re}(\alpha_\pm,\beta)\geqslant 0$ in planes cut along $\mathrm{Im}(r)=0$, $|\,\mathrm{Re}(r)\,|>(b_\pm,b)$, respectively, and it can be shown that

$$m_+>1>m_-(b_+>a>b_-),\quad \tau>0 \tag{10a}$$

$$m_+>m(b_+>b),\quad 0<\tau<\tau_m;\quad \tau_m=\frac{m^2(1+\varepsilon)-1}{m^2(m^2-1)} \tag{10b}$$

and, therefore, that

$$M_+ > 0 > M_-, \quad \lambda_- > 0 > \lambda_+ \tag{11}$$

for all $\tau > 0$. Comparison of (7) with corresponding classical 3D transient results (Brock, 1981) shows that all field variables except the temperature change ω exhibit both rotational waves (β-exponential terms) and signals ($\alpha_\pm$-exponential terms) that are not—because of the dependence of the branch points $b_\pm$ on the temporal transform parameter s—classical waves.

Application of (6a, b) to (3) in view of (2) and (5) gives the equation set

$$\begin{bmatrix} -\lambda_+\alpha_+ & -\lambda_-\alpha_- & 0 & 0 \\ 2p\alpha_+ & 2p\alpha_- & -T_q & pq \\ 2q\alpha_+ & 2q\alpha_- & pq & -T_p \\ T & T & 2p\beta & 2q\beta \end{bmatrix} \begin{bmatrix} A_+ \\ A_- \\ \frac{1}{\beta}B_x \\ \frac{1}{\beta}B_y \end{bmatrix} = \begin{bmatrix} \frac{1}{s}F^* \\ \frac{1}{\mu}\tau_x^* \\ \frac{1}{\mu}\tau_y^* \\ \frac{-1}{\mu}\sigma^* \end{bmatrix} \tag{12}$$

for $(A_\pm, \mathbf{B})$ in the half-space $z > 0$. These functions, and, therefore, the expressions for the solutions transforms $(\mathbf{u}^*, \sigma^*, \omega^*)$, will all exhibit in their denominators the determinant

$$R = (\lambda\alpha)_+ R_- - (\lambda\alpha)_- R_+ \tag{13}$$

of the coefficient matrix of (12), where

$$R_\pm = 4r^2\alpha_\pm\beta + T^2. \tag{14}$$

Here, R is the thermoelastic Rayleigh function, and its zeroes are now studied.

RAYLEIGH SIGNAL: ANALYSIS OF ZEROES

Equation (13) shows that R is a function not of $\mathbf{p}$, but of its scalar resultant r, and is, therefore, identical in form to the corresponding 2D result (Brock, 1995), where the scalar is then a specific transform variable (with respect to x, say). Indeed, the forms of $R_\pm$ are similar in form to the classical Rayleigh function (Achenbach, 1973) in a 2D transient study. The zeroes of R in the thermal 2D case produce pole-type singularities for $(\mathbf{u}^*, \sigma^*, \omega^*)$ in the complex plane of the spatial transform variable (Brock, 1992, 1993) which for positive real s lie on the real axis. Because transform inversion involves integrations in the plane that passes near the singularities as $z \to 0$, residues and Cauchy principal value integral contributions to the functions $(\mathbf{u}, \sigma, \omega)$ themselves are produced, which may dominate their surface behavior. Analogous considerations arise, of course, in classical 2D wave propagation studies (Achenbach, 1973; Miklowitz, 1978; Brock, 1982b). While r is a scalar resultant of two transform variables (p, q), we proceed by analogy with 2D studies and seek the zeroes of R in the complex r-plane. The role of these zeroes in solution behavior is illustrated in a later section.

The function R is analytic in the r-plane cut along $\mathrm{Im}(r) = 0$, $|\mathrm{Re}(r)| > b_-$, and finite in this cut plane for finite $|r|$. The argument principle (Hille, 1959) implies, therefore, that the number of zeroes of R in the cut plane is equal to the net number of times that traversing a simple contour about the entire cut plane produces a circuit of the origin in the ζ-plane in the same sense under the mapping

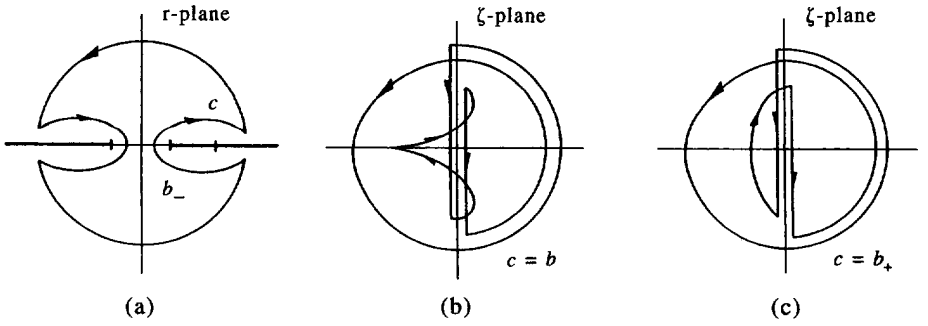

Fig. 1. (a) Contour for cut r-plane. (b) ζ-plane mapping for $c = b$. (c) ζ-plane mapping for $c = b_+$.

$$\zeta = R(r). \tag{15}$$

Such a contour is shown schematically in Fig. 1a, where it is understood that the circular part has an infinite radius and that the curves surrounding the branch cuts $\mathrm{Im}(r) = 0$, $|\mathrm{Re}(r)| > b_-$ collapse onto those cuts. In view of (10), (11), (12) and (13) it can be shown that $R(0)$ and $R(b_-)$ are real and negative and that $R(c)$ is a positive imaginary number, where

$$c = \max(b, b_+). \tag{16}$$

Moreover,

$$R \approx \pm i2(\lambda_+ - \lambda_-)(a^2 - b^2)r^3, \quad |r| \to \infty \tag{17}$$

where $\pm$ denotes $\mathrm{Im}(r) < 0$ and $\mathrm{Im}(r) > 0$, respectively. This information can be used to show that a mapping (15) of one circuit about the contour in Fig. 1a produces two circuits about the contour shown schematically in Fig. 1b, c for $c = b$ and $c = b_+$, respectively. The mapping in neither case completely circles the origin in the ζ-plane, so that R has no zeroes in the cut r-plane. However, these same mappings indicate that R is imaginary in the infinite intervals $\mathrm{Im}(r) = 0$, $|\mathrm{Re}(r)| > c$ and always changes sign as $|r| \to \infty$. Because it is an even function, therefore, R exhibits two non-isolated zeroes of the form

$$r = \pm b_o \tag{18}$$

on its branch cuts. To obtain these, the function

$$G = \frac{R}{2(\lambda_+ - \lambda_-)(a^2 - b^2)(r^2 - b_o^2)\sqrt{c^2 - r^2}} \tag{19}$$

is introduced, which is analytic in the plane cut along $\mathrm{Im}(r) = 0$, $b_- < |\mathrm{Re}(r)| < c$, has no zeroes in the cut plane, exhibits only an integrable singularity at the branch points $r = \pm c$, and approaches unity as $|r| \to \infty$. It can, therefore, be written as the product of two functions $G_\pm$ that are analytic in the overlapping half-planes $\mathrm{Re}(r) > -b_-$ and $\mathrm{Re}(r) < b_-$, respectively. These functions can be obtained by a product-splitting operation (Noble, 1958) as

$$\ln G_\pm = -\frac{1}{\pi}\int_{b_-}^{c} \tan^{-1}\frac{\mathrm{Im}(R)}{\mathrm{Re}(R)}\frac{\mathrm{d}u}{u \pm r} \tag{20}$$

where $R(u)$ is evaluated along the upper side of the branch cut. More explicitly, we have

$$\ln G_{\pm} = -\frac{1}{\pi}\left(\int_{b_-}^{b_+} \tan^{-1} B_o + \int_{b_+}^{b} \tan^{-1} C\right)\frac{du}{u \pm r} \quad (c = b) \tag{21a}$$

$$\ln G_{\pm} = -\frac{1}{\pi}\left(\int_{b_-}^{b} \tan^{-1} B_o + \int_{b}^{b_+} \tan^{-1} C_+\right)\frac{du}{u \pm r} \quad (c = b_+) \tag{21b}$$

where now

$$B_o = \frac{4\lambda_+ u^2 A_- \beta}{\lambda_- R_+ - \lambda_- T^2}, \quad C = \frac{4u^2\beta[(\lambda\alpha)_- - (\lambda\alpha)_+]}{T^2(\lambda_+ - \lambda_-)}, \quad C_+ = \frac{4\lambda_- u^2 \alpha_+ B}{\lambda_+ R_- - \lambda_- T^2} \tag{22a}$$

$$A_{\pm} = \sqrt{u^2 - b_{\pm}^2}, \quad B = \sqrt{u^2 - b^2}. \tag{22b}$$

Equations (21) show that $G_-(0) = G_+(0)$, so that setting $r = 0$ in (19) gives

$$b_o = \frac{b^2}{\sqrt{2(b^2 - a^2)}} \frac{1}{G_+(0)} \sqrt{\frac{a}{c} \frac{m_+ M_+ - m_- M_-}{M_+ - M_-}}. \tag{23}$$

The dependence of b_o on the temporal transform variable s through the dimensionless parameter τ in $b_{\pm}$ is noted.

The role of this zero and the influence of thermoelastic Rayleigh signals on transient surface response is, as noted above, considered later. At present, the zeroes arising in a Stoneley signal problem are studied.

A STONELEY SIGNAL PROBLEM

Consider two half-spaces rigidly joined along an interface defined in terms of $\mathbf{x}$ as $z = 0$. All parameters and field variables in the half-space $z > 0$ carry the subscript 1, while those for $z < 0$ have the subscript 2. For time $t \leqslant 0$ the half-spaces are at rest at a uniform temperature $T_o(K)$. For $t > 0$ a temperature field is prescribed over the interface, as are discontinuities in the displacement and traction fields. The governing equations for each half-space are again (2) and (5), now appropriately subscripted, while for $z = 0$, $t > 0$ we now have

$$[\mathbf{u}] = \mathbf{U}, \quad [\sigma \cdot \mathbf{k}] = (\tau_x, \tau_y, \sigma), \quad \omega_1 = \omega_2 = \Omega \tag{24}$$

where [ ] denotes a jump in a quantity in traveling from half-space $z < 0$ (2) to half-space $z > 0$ (1). Here (τ_x, τ_y, σ), $\mathbf{U} = (U, V, W)$ and Ω are piecewise continuous functions of (ρ, t) and bounded in ρ for finite $t > 0$. Therefore, $(\mathbf{u}_1, \mathbf{u}_2, \omega_1, \omega_2)$ should also be bounded for finite $t > 0$ and continuous in $(\mathbf{x}, t)$ in their respective half-spaces. Use of (6) produces again the formulas (7)–(11), with proper subscripting added. The transforms of the interface conditions (24) then give the equation set

$$\begin{bmatrix} \mathbf{C}_1 & \mathbf{C}_2 \\ \mathbf{D}_1 & \mathbf{D}_2 \end{bmatrix} \begin{bmatrix} \mathbf{A}_1 \\ \mathbf{A}_2 \end{bmatrix} = [\mathbf{F}] \tag{25}$$

for the unknown functions $(A_{1\pm}, A_{2\pm}, \mathbf{B}_1, \mathbf{B}_2)$ of $(s, \mathbf{p})$. Here $\mathbf{A}_i$ $(i = 1, 2)$ and $\mathbf{F}$ are column matrices with elements $(A_{i+}, A_{i-}, 1/\beta_i B_{ix}, 1/\beta_i B_{iy})$ and $(\Omega^*, \Omega^*, sU^*, sV^*, sW^*, \tau_x^*, \tau_y^*, \sigma^*)$, respectively, $(\mathbf{C}_1, \mathbf{D}_1)$ are the square matrices

$$\mathbf{C}_1 = \begin{bmatrix} \lambda_{1+} & \lambda_{1-} & 0 & 0 \\ 0 & 0 & 0 & 0 \\ -p & -p & \beta_1 & 0 \\ -q & -q & 0 & \beta_1 \end{bmatrix}, \quad \mathbf{D}_1 = \begin{bmatrix} \alpha_{1+} & \alpha_{1-} & p & q \\ 2p(\mu\alpha_+)_1 & 2p(\mu\alpha_-)_1 & -(\mu T_q)_1 & \mu_1 pq \\ 2q(\mu\alpha_+)_1 & 2q(\mu\alpha_-)_1 & \mu_1 pq & -(\mu T_p)_1 \\ -(\mu T)_1 & -(\mu T)_1 & -2p(\mu\beta)_1 & -2q(\mu\beta)_1 \end{bmatrix} \tag{26}$$

while $(\mathbf{C}_2, \mathbf{D}_2)$ are the square matrices

$$\mathbf{C}_2 = \begin{bmatrix} 0 & 0 & 0 & 0 \\ \lambda_{2+} & \lambda_{2-} & 0 & 0 \\ p & p & -\beta_2 & 0 \\ q & q & 0 & -\beta_2 \end{bmatrix},$$

$$\mathbf{D}_2 = \begin{bmatrix} \alpha_{2+} & \alpha_{2-} & p & q \\ 2p(\mu\alpha_+)_2 & 2p(\mu\alpha_-)_2 & -(\mu T_q)_2 & \mu_2 pq \\ 2q(\mu\alpha_+)_2 & 2q(\mu\alpha_-)_2 & \mu_2 pq & -(\mu T_p)_2 \\ (\mu T)_2 & (\mu T)_2 & 2p(\mu\beta)_2 & 2q(\mu\beta)_2 \end{bmatrix}. \tag{27}$$

One can introduce the parameters (Cagniard, 1962)

$$c_1 = \frac{\mu_1}{2(\mu_1 - \mu_2)}, \quad c_2 = \frac{1}{2} - c_1 = \frac{\mu_2}{2(\mu_2 - \mu_1)}, \quad \Omega_1 = c_1 b_1^2, \quad \Omega_2 = c_2 b_2^2 \tag{28}$$

and obtain from the determinant of the square matrix in (25) the Stoneley function

$$S = -\lambda_{1+}\lambda_{2+}S_- + \lambda_{1+}\lambda_{2-}S_\pm + \lambda_{1-}\lambda_{2+}S_\pm - \lambda_{1-}\lambda_{2-}S_+. \tag{29}$$

In (29)

$$\frac{S_\pm}{4(\mu_1 - \mu_2)^2} = r^2(\alpha_{1-}\beta_1\alpha_{2+}\beta_2 + P_{12}^2) + \alpha_{1-}\beta_1 P_2^2 + \alpha_{2+}\beta_2 P_1^2 - \Omega_1\Omega_2(\alpha_{1-}\beta_2 + \alpha_{2+}\beta_1) \tag{30a}$$

$$P_1 = \Omega_1 - r^2, \quad P_2 = \Omega_2 - r^2, \quad P_{12} = \Omega_1 + \Omega_2 - r^2 \tag{30b}$$

and (S_+, S_-) follow by making both subscripts $(+, -)$, respectively, while $S_\mp$ follows by switching the $(+, -)$-subscripts. It should be noted that the subscripted S-functions all have the same form as the Stoneley function for a 2D classical problem (Cagniard, 1962) where, of course, r is then a single transform variable. In view of this, we adopt the viewpoint used for the Rayleigh signal case and seek the zeroes of S in the complex r-plane.

From (8), (10), (11) and (30), it can be seen that S is analytic in the r-plane cut along $\mathrm{Im}(r) = 0$, $c_- < |\,\mathrm{Re}(r)\,| < c_+$, where

$$c_- = \min(b_{1-}, b_{2-}), \quad c_+ = \max(b_1, b_{1+}, b_2, b_{2+}). \tag{31}$$

To study the possible zeroes of S, the argument principle (Hille, 1959) is employed with the mapping

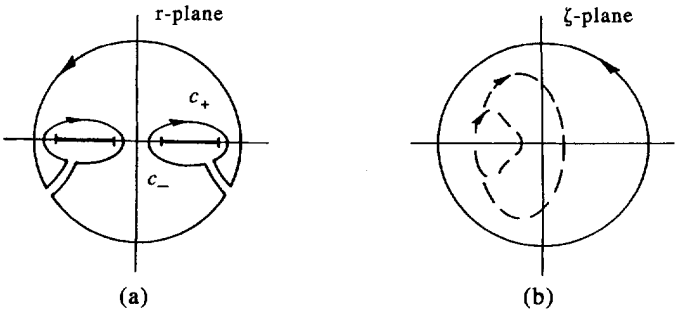

Fig. 2. (a) Contour for cut r-plane. (b) ζ-plane mapping.

$$\zeta = S(r) \tag{32}$$

and the contour shown schematically in Fig. 2a. Despite the many magnitude-based orderings of $(b_1, b_{1\pm}, b_2, b_{2\pm})$ possible, it can be shown that

$$\frac{S}{2(\mu_1-\mu_2)^2} \approx -(\lambda_{1+}-\lambda_{1-})(\lambda_{2+}-\lambda_{2-})(4\Omega_1-a_1^2-b_1^2)(4\Omega_2-a_2^2-b_2^2)r^2, \quad |r| \to \infty \tag{33}$$

and that $S(0)$ and $S(c_-)$ are real and positive. The quantity $S(c_+)$ is also real, but its sign depends on the particular combination of parameters $(b_1, b_{1\pm}, b_2, b_{2\pm}, \lambda_{1\pm}, \lambda_{2\pm}, \Omega_1, \Omega_2)$. Therefore, in a manner analogous to that for the Rayleigh signal case, the mapping (32) takes one trip about the contour in Fig. 2a into two circuits about the contour shown schematically in Fig. 2b. The dashed lines indicate the two possibilities: if $S(c_+) < 0$, the mapping will circle the origin in the ζ-plane twice, while if $S(c_+) > 0$, then circuits by the inner and outer contours are in opposite directions. Because S is even in r and is, as (33) shows, positive as $|r| \to \infty$, the two zeroes

$$r = \pm b_o, \quad b_o > c_+ \tag{34}$$

occur in the cut plane when $S(c_+) < 0$. To obtain these zeroes, the function

$$G = \frac{-S}{2(\mu_1-\mu_2)^2(\lambda_{1+}-\lambda_{1-})(\lambda_{2+}-\lambda_{2-})(4\Omega_1-a_1^2-b_1^2)(4\Omega_2-a_2^2-b_2^2)(r^2-b_o^2)} \tag{35}$$

is introduced. It is analytic, has no zeroes in the cut plane of S and approaches unity as $|r| \to \infty$. The same product-splitting operations used previously can be applied, therefore, to find functions $G_\pm$ that are analytic in the overlapping half-planes $\mathrm{Re}(r) > -c_-$, $\mathrm{Re}(r) < c_-$:

$$\ln G_\pm = -\frac{1}{\pi}\int_{c_-}^{c_+} \tan^{-1}\frac{\mathrm{Im}(S)}{\mathrm{Re}(S)}\frac{du}{u \pm r}. \tag{36}$$

Here $S(u)$ is evaluated along the upper side of the branch cut. Little insight is gained by giving explicit forms for (36) for all possible orderings of $(b_1, b_{1\pm}, b_2, b_{2\pm})$ but, as an example, we present the results for the case $b_{1-} < b_{2-} < b_1 < b_2 < b_{1+} < b_{2+}$, $S(b_{2+}) < 0$:

$$\ln G_{\pm} = -\frac{1}{\pi}\left(\int_{b_{1-}}^{b_{2-}} \tan^{-1} B_o^- + \int_{b_{2-}}^{b_1} \tan^{-1} C_- + \int_{b_1}^{b_2} \tan^{-1} D\right)\frac{du}{u \pm r}$$
$$-\frac{1}{\pi}\left(\int_{b_2}^{b_{1+}} \tan^{-1} B_o^+ + \int_{b_{1+}}^{b_{2+}} \tan^{-1} C_+\right)\frac{du}{u \pm r}. \tag{37}$$

In (37) the inverse tangent arguments are ratios and the numerator/denominator pairs are

$$\lambda_{1+}A_{1-}[(\lambda_{2+}-\lambda_{2-})(\beta_1 P_2^2 - \Omega_1\Omega_2\beta_2) + u^2\beta_1\beta_2(\lambda_{2+}\alpha_{2-} - \lambda_{2-}\alpha_{2+})],$$
$$\lambda_{1+}[(\lambda_{2-}-\lambda_{2+})u^2P_{12}^2 + (\lambda_{2-}\alpha_{2+} - \lambda_{2+}\alpha_{2-})(\beta_2 P_1^2 - \Omega_1\Omega_2)] \tag{38a}$$
$$+\frac{\lambda_{1-}}{4(\mu_1-\mu_2)^2}(\lambda_{2+}S_{\mp} - \lambda_{2-}S_+)$$

$$\lambda_{1+}\lambda_{2+}[A_{1-}(\beta_1 P_2^2 - \Omega_1\Omega_2\beta_2) + A_{2-}(\beta_2 P_1^2 - \Omega_1\Omega_2\beta_1)]$$
$$+\lambda_{1+}\lambda_{2-}A_{1-}(\Omega_1\Omega_2\beta_2 - \beta_1 P_2^2 - u^2\beta_1\alpha_{2+}\beta_2) + \lambda_{1-}\lambda_{2+}A_{2-}(\Omega_1\Omega_2\beta_1 - \beta_2 P_1^2 - u^2\beta_2\alpha_{1+}\beta_1),$$
$$+\lambda_{1+}\lambda_{2-}(u^2P_{12}^2 + \alpha_{2+}\beta_2 P_1^2 - \Omega_1\Omega_2\alpha_{2+}\beta_1) + \lambda_{1-}\lambda_{2+}(u^2P_{12}^2 + \alpha_{1+}\beta_1 P_2^2 - \Omega_1\Omega_2\alpha_{1+}\beta_2)$$
$$+\lambda_{1+}\lambda_{2+}u^2(A_{1-}\beta_1 A_{2-}\beta_2 - P_{12}^2) - \frac{1}{4(\mu_1-\mu_2)^2}\lambda_{1-}\lambda_{2-}S_+ \tag{38b}$$

$$\lambda_{1+}\lambda_{2+}\beta_2(A_{2-}P_1^2 - u^2A_{1-}B_1A_{2-} - \Omega_1\Omega_2A_{1-}) + \lambda_{1-}\lambda_{2-}B_1(u^2\alpha_{1+}\alpha_{2+}\beta_2 + \alpha_{1+}P_2^2 - \Omega_1\Omega_2\alpha_{2+})$$
$$+\lambda_{1+}\lambda_{2-}\Omega_1\Omega_2(A_{1-}\beta_2 + \alpha_{2+}B_1) - \lambda_{1-}\lambda_{2+}(\alpha_{1+}B_1P_2^2 + A_{2-}\beta_2P_1^2),$$
$$\lambda_{1+}\lambda_{2+}(u^2P_{12}^2 + A_{1-}\beta_1P_2^2 - \Omega_1\Omega_2A_{2-}B_1) + \lambda_{1-}\lambda_{2-}(\Omega_1\Omega_2\alpha_{1+}\beta_2 - \alpha_{2+}\beta_2P_1^2 - u^2P_{12}^2)$$
$$+\lambda_{1+}\lambda_{2-}[\alpha_{2+}\beta_2P_1^2 - A_{1-}B_1P_2^2 + u^2(P_{12}^2 - A_{1-}B_1\alpha_{2+}\beta_2)]$$
$$+\lambda_{1-}\lambda_{2+}[\Omega_1\Omega_2(A_{2-}B_1 - \alpha_{2+}\beta_2) + u^2(P_{12}^2 - \alpha_{1+}B_1A_{2-}\beta_2)] \tag{38c}$$

$$\lambda_{1+}\lambda_{2-}\alpha_{2+}(u^2A_{1-}B_1B_2 + \Omega_1\Omega_2B_1 - B_2P_1^2) + \lambda_{1-}\lambda_{2+}\alpha_{1+}(u^2B_1A_{2-}B_2 + \Omega_1\Omega_2B_2 - B_1P_2^2)$$
$$+\lambda_{1-}\lambda_{2-}[\alpha_{1+}B_1P_2^2 + \alpha_{2+}B_2P_1^2 - \Omega_1\Omega_2(\alpha_{1+}B_2 + \alpha_{2+}B_1)],$$
$$\lambda_{1+}\lambda_{2+}[u^2(A_{1-}B_1A_{2-}B_2 + P_{12}^2) + A_{1-}B_1P_2^2 + A_{2-}B_2P_1^2 - \Omega_1\Omega_2(A_{1-}B_2 + A_{2-}B_1)]$$
$$+\lambda_{1+}\lambda_{2-}(\Omega_1\Omega_2A_{1-}B_2 + u^2P_{12}^2 - A_{1-}B_1P_2^2) + \lambda_{1-}\lambda_{2+}(\Omega_1\Omega_2A_{2-}B_1 - A_{2-}B_2P_1^2)$$
$$+\lambda_{1-}\lambda_{2-}u^2(\alpha_{1+}B_1\alpha_{2+}B_2 - P_{12}^2) \tag{38d}$$

$$\lambda_{2-}\alpha_{2+}[(\lambda_{1+}-\lambda_{1-})(\Omega_1\Omega_2B_1 - B_2P_1^2) + u^2B_1B_2(\lambda_{1+}A_{1-} - \lambda_{1-}A_{1+})],$$
$$\lambda_{1+}\lambda_{2+}[u^2(A_{1-}B_1A_{2-}B_2 + P_{12}^2) + A_{1-}B_1P_2^2 + A_{2-}B_2P_1^2 - \Omega_1\Omega_2(A_{1-}B_2 + A_{2-}B_1)]$$
$$+\lambda_{1-}\lambda_{2+}[u^2(A_{1+}B_1A_{2-}B_2 + P_{12}^2) + \Omega_1\Omega_2(A_{1+}B_2 + A_{2-}B_1) - A_{1+}B_1P_2^2 - A_{2-}B_2P_1^2]$$
$$+\lambda_{1+}\lambda_{2-}(u^2P_{12}^2 + \Omega_1\Omega_2A_{1-}B_2 - A_{1-}B_1P_2^2) + \lambda_{1-}\lambda_{2-}(u^2P_{12}^2 + A_{1+}B_1P_2^2 - \Omega_1\Omega_2A_{1+}B_2) \tag{38e}$$

for $(B_o^-, C_-, D, B_o^+, C_+)$, respectively. In (38) the eqns (22b) hold, with the appropriate subscripts attached. Setting $r = 0$ in (35) now gives

$$b_o = \frac{1}{G_+(0)}$$
$$\times \sqrt{\frac{2(\Omega_2b_1 - \Omega_1b_2)}{(4\Omega_1 - a_1^2 - b_1^2)(4\Omega_2 - a_2^2 - b_2^2)}}\left[\frac{\Omega_2a_1(1+m_{1+}m_{1-})}{m_{1+}+m_{1-}} - \frac{\Omega_1a_2(1+m_{2+}m_{2-})}{m_{2+}+m_{2-}}\right]. \tag{39}$$

With these results available, we now examine the effects of thermoelastic Rayleigh/Stoneley signals in terms of simple examples for the Rayleigh signal case.

RAYLEIGH SIGNAL ILLUSTRATION

We solve (12) in light of (13) for the coefficient $(A_{\pm}, \mathbf{B})$ and substitute them into (7a) in order to obtain the transform

$$R\omega_o^* = \frac{F^*}{s}(\lambda_- R_+ - \lambda_+ R_-) + \lambda_+\lambda_-\left(T\frac{\sigma^*}{\mu} - 2p\beta\frac{\tau_x^*}{\mu} - 2q\beta\frac{\tau_y^*}{\mu}\right)(\alpha_- - \alpha_+) \tag{40}$$

for the temperature change ω_o on the half-space surface $z = 0$. Now consider the specific case of a half-space subject to a normal traction with uniform value σ_o distributed over a surface disk of fixed radius ρ_o centered at the origin. Then

$$\sigma = \sigma_o \ (\rho < \rho_o), \quad \tau_x = \tau_y = F = 0 \tag{41}$$

where now $\rho = \sqrt{x^2 + y^2}$. Operating on (41) with (6) gives

$$\sigma^* = \frac{2\pi\sigma_o}{s^2 r}\rho_o I_1(sr\rho_o), \quad \tau_x^* = \tau_y^* = F^* = 0 \tag{42}$$

where I_1 is the MacDonald function of order 1 (Watson, 1966). The inverse operation of (6b) is (van der Pol and Bremmer, 1950)

$$\hat{f}(\mathbf{x}) = \left(\frac{s}{2\pi i}\right)^2 \iint f^* \, \mathrm{e}^{s(\mathbf{p}\cdot\boldsymbol{\rho})} \, \mathrm{d}p \, \mathrm{d}q \tag{43}$$

where integration in the complex (p, q)-planes can here be taken along the respective imaginary axes. The exponential argument in (43) suggests the transform variable rotation (Norwood, 1977)

$$\mathbf{p}\cdot\boldsymbol{\rho} = xp + yq = P\rho, \quad yp - xq = Q\rho, \quad \sqrt{P^2 + Q^2} = \sqrt{p^2 + q^2} = r \tag{44}$$

with Jacobian of unity. Substitution of (40) into (43) in view of (44) under the assumption that the resulting (P, Q)-integrations can also be taken along the respective imaginary axes gives the single transform

$$\hat{\omega}_o = -\rho_o \frac{\sigma_o}{\mu}\lambda_+\lambda_- \int_0^\infty \mathrm{d}v \frac{1}{\pi i}\int \mathrm{e}^{sP\rho}\frac{T}{rR}(\alpha_- - \alpha_+) I_1(sP\rho_o)\,\mathrm{d}P \tag{45}$$

where P-integration is along the imaginary axis, ω_o^* has been recognized as an even function of Q and the substitution $Q = iv$, $v > 0$ made. In (45), therefore,

$$r = \sqrt{P^2 - v^2} \tag{46}$$

and $(\alpha_{\pm}, \beta)$ can now be viewed as functions with positive real parts that are analytic in the P-plane cut along $\mathrm{Im}(P) = 0, |\mathrm{Re}(P)| > (\sqrt{b_{\pm}^2 + v^2}, \sqrt{b^2 + v^2})$, respectively. Similarly, the function R can now be said to, in light of (23), exhibit zeroes on its branch cuts $\mathrm{Im}(P) = 0, |\mathrm{Re}(P)| > \sqrt{b_-^2 + v^2}$ at

$$P = \pm B_o, \quad B_o = \sqrt{b_o^2 + v^2}. \tag{47}$$

A numerical inversion scheme could now be employed to obtain ω_o, but in the present study, interest is on the contributions associated with the Rayleigh signals. To illustrate their behavior, a long-time analytical solution is sufficient.

The Tauberian theorems imply that inverting an asymptotic expression for a unilateral Laplace transform valid for small s will give a function valid for large t. Equation (8) shows that the Rayleigh/Stoneley functions (13) and (29) depend on s through the dimensionless parameters τ and (τ_1, τ_2). In (8), however, the factor ah is quite small, e.g., $O(10^{-14})$ s for a steel-like material (Brock, 1992), because the thermoelastic characteristic lengths h and (h_1, h_2) are themselves small. Therefore, the use of small-τ approximations in the solution transforms may actually not place much of a restriction on the solutions themselves. Thus, the asymptotic expressions

$$m_+ \approx \sqrt{\frac{1+\varepsilon}{\tau}}, \quad m_- \approx \frac{1}{\sqrt{1+\varepsilon}} \tag{48}$$

are introduced, and only the lowest-order terms in τ and (τ_1, τ_2) kept. The result is that the terms (R_-, S_-) effectively become the Rayleigh/Stoneley functions in (13) and (29). The form of R_-, in particular, agrees with the low-frequency function obtained by Chadwick (1960) and Nowinski (1978). Then, (23) reduces to

$$b_o = \frac{b^2}{\sqrt{2(b^2 - a^2)}} \frac{1}{G_+(0)} \tag{49}$$

where now

$$\ln G_\pm = -\frac{1}{\pi} \int_{b_-}^{b} \tan^{-1} C \frac{du}{u \pm r}, \quad C = \frac{4u^2 A_- \beta}{T^2}, \quad b_- = \frac{a}{\sqrt{1+\varepsilon}}. \tag{50}$$

Although not of use here, for completeness we give the corresponding result

$$b_o = \frac{1}{G_+(0)} \sqrt{\frac{2(\Omega_2 b_1 - \Omega_1 b_2)(\Omega_2 b_{1-} - \Omega_1 b_{2-})}{(4\Omega_1 - a_1^2 - b_1^2)(4\Omega_2 - a_2^2 - b_2^2)}} \tag{51}$$

for (39), where, for the case illustrated, (37) and (38) reduce to

$$\ln G_\pm = -\frac{1}{\pi} \left(\int_{b_{1-}}^{b_{2-}} \tan^{-1} C_- + \int_{b_{2-}}^{b_1} \tan^{-1} C + \int_{b_1}^{b_2} \tan^{-1} C_+ \right) \frac{du}{u \pm r} \tag{52}$$

and

$$C_- = A_{1-} \frac{\Omega_1 \Omega_2 \beta_2 - \beta_1 P_2^2 - u^2 \beta_1 \alpha_{2-} \beta_2}{u^2 P_{12}^2 + \alpha_{2-} \beta_2 P_1^2 - \Omega_1 \Omega_2 \alpha_{2-} \beta_1} \tag{53a}$$

$$C = \frac{\Omega_1 \Omega_2 (A_{1-} \beta_2 + A_{2-} \beta_1) - A_{1-} \beta_1 P_2^2 - A_{2-} \beta_2 P_1^2}{u^2 (P_{12}^2 - A_{1-} \beta_1 A_{2-} \beta_2)} \tag{53b}$$

$$C_+ = \beta_2 \frac{u^2 A_{1-} B_1 A_{2-} + \Omega_1 \Omega_2 A_{1-} - A_{2-} P_1^2}{u^2 P_{12}^2 + \Omega_1 \Omega_2 A_{2-} B_1 - A_{1-} B_1 P_2^2} \tag{53c}$$

under the restriction

$$\sqrt{b_2^2-b_1^2}[\Omega_1\Omega_2\sqrt{b_2^2-b_{2-}^2}-(\Omega_2-b_2^2)^2\sqrt{b_2^2-b_{1-}^2}]+b_2^2(\Omega_1+\Omega_2-b_2^2)^2<0. \quad (54)$$

Returning now to the contribution of the Rayleigh signal, we proceed by analogy with classical 2D studies (Achenbach, 1973; Miklowitz, 1978) and recognize that (47) defines poles for the integrand of (45). Therefore, the non-exponential part of this integrand is replaced by an expression valid near $P = \pm B_o$ ($r = \pm b_o$). In particular, the function R can be approximated by the form

$$2(\lambda_+-\lambda_-)(a^2-b^2)\sqrt{c^2-b_o^2}G_+(b_o)G_-(b_o)(P^2-B_o^2) \quad (55)$$

obtained from (19), where it is noted that the long-time expressions (50) for $G_\pm$ are analytic at $P = \pm B_o$ because it can be shown that now $b_o > b$. Use of (48) gives the forms

$$\alpha_+ \approx \sqrt{\left(\frac{1+\varepsilon}{hs}\right)^2-b_o^2}, \quad \alpha_- = \pm iA_-, \quad A_- \approx \sqrt{b_o^2-\left(\frac{a}{1+\varepsilon}\right)^2}, \quad c \approx \sqrt{\frac{1+\varepsilon}{hs}} \quad (56)$$

for (45), where the (+)-sign arises in the second and fourth quadrants of the P-plane, and the (−)-sign, in the other two quadrants. In view of Cauchy residue theory, the P-integration in (45) can then be replaced by an integration along the upper and lower sides of the negative Re(P)-axis in opposite directions. The result is that (45) takes the approximate form

$$\hat{\omega_o} \approx \frac{b^2\rho_o I_1(sb_o\rho_o)T(b_o)}{(M_+-M_-)(a^2-b^2)G_+(b_o)G_-(b_o)\alpha_+ b_o}\frac{\varepsilon}{\kappa\tau}\frac{\sigma_o}{\mu}$$
$$\times\int_0^\infty dv\left(\frac{1}{\pi}A_-\int_0^\infty e^{-su\rho}\frac{du}{u^2-B_o^2}-\frac{\alpha_+}{2B_o}e^{-sB_o\rho}\right) \quad (57)$$

where (8d) has been used and u now plays the role of P. Equations (8), (48) and (56) indicate that the second term in (57) dominates as $s \to 0$ and, indeed, behaves as

$$e^{-sB_o\rho}I_1(sb_o\rho_o), \quad s \approx 0. \quad (58)$$

The inverse of (58) is (Abramowitz and Stegun, 1972)

$$\frac{B_o\rho-t}{\pi b_o\rho_o}\frac{1}{\sqrt{b_o^2\rho_o^2-(t-B_o\rho)^2}} \quad (B_o\rho > b_o\rho_o > |t-B_o\rho|) \quad (59)$$

so that, upon making the integration variable change $v = \sqrt{u^2-b_o^2}, u > b_o$ in (57), we obtain

$$\omega_o \approx \frac{\varepsilon}{1+\varepsilon}\frac{\sigma_o}{\pi\mu\kappa}\frac{b^2}{a^2-b^2}\frac{T(b_o)}{2b_o^2G_+(b_o)G_-(b_o)}\int_{u_-}^{u_+}\frac{t-u\rho}{\sqrt{b_o^2\rho_o^2-(t-u\rho)^2}}\frac{du}{\sqrt{u^2-b_o^2}} \quad (u_+ > u_-) \quad (60a)$$

$$u_+ = \frac{t+b_o\rho_o}{\rho}, \quad u_- = \max\left(b_o, \frac{b_o\rho_o}{\rho}, \frac{t-b_o\rho_o}{\rho}\right). \quad (60b)$$

The integral in (60a) can be replaced by a combination of elliptic integrals of the first and third kinds (Gradshteyn and Ryzhik, 1975). Their moduli and arguments depend on u_-,

however, and as the classical results of Brock (1980) for pressure loading over a non-uniformly expanding surface area show, the present form is actually more efficient for calculations.

This problem displays axial symmetry, so, as truer 3D examples, consider normal surface tractions imposed over the same surface disk of radius ρ_o in such a manner that the net normal forces vanish, i.e., surface bending couples are the resultant:

$$\sigma = \sigma_o(\cos\theta, \sin\theta)\ (\rho < \rho_o), \quad \tau_x = \tau_y = F = 0. \tag{61}$$

Here, $\tan\theta = y/x$ and operation on (61) with (6a, b) gives

$$\sigma^* = -\rho_o^2 \frac{\sigma_o}{s^2 r^2 \rho}(P, Q)\left[I_o(sr\rho_o) - \frac{I_1(sr\rho_o)}{sr\rho_o}\right], \quad \tau_x^* = \tau_y^* = F^* = 0 \tag{62}$$

where I_o is the MacDonald function of order 0 (Watson, 1966). Carrying out the same inversion procedure then gives

$$\omega_o \approx \frac{\varepsilon}{1+\varepsilon}\frac{\sigma_o}{\pi\mu\kappa}\frac{b^2}{b^2-a^2}\frac{T(b_o)(\cos\theta, \sin\theta)}{2b_0^4 G_+(b_o)G_-(b_0)\rho}\int_{u_-}^{u_+}\frac{(t-u\rho)^2}{\sqrt{b_o^2\rho_o^2-(t-u\rho)^2}}\frac{u\,du}{\sqrt{u^2-b_o^2}}\ (u_+ > u_-). \tag{63}$$

Equation (63) preserves in ω_o the θ-dependence of the imposed normal traction.

SOME NUMERICAL RESULTS

Equations (49) and (51) indicate that, for long times, the Rayleigh/Stoneley zeroes b_o are constants. That is, their inverses are the Rayleigh/Stoneley signal speeds, v_R and v_S, respectively. Their values are essentially the classical values, modified by the thermoelastic factors $\sqrt{1+\varepsilon}$ and $(\sqrt{1+\varepsilon_1}, \sqrt{1+\varepsilon_2})$. Table 1 presents values of v_R for three materials, and Table 2 presents values of v_S for those combinations of the materials for which v_S exists.

To illustrate the surface temperature change induced for long times by the Rayleigh signal, ω_o given by (60) and the amplitude $|\omega_o|$ obtained from (63) are plotted in Figs 3

Table 1.

	ν	ρ (kg/m^3)	μ (GPa)	ε	v_R (m/s)
aluminum	0.33	2768	25.9	0.036	2857
stnls stl.	0.3	7778	73.1	0.0071	2842
titanium	0.34	4512	41.4	0.009	2826

Table 2.

	v_{R1} (m/s)	v_{R2} (m/s)	v_S (m/s)
aluminum (1) stnls stl. (2)	2857	2842	3026
aluminum (1) titanium (2)	2857	2826	3027

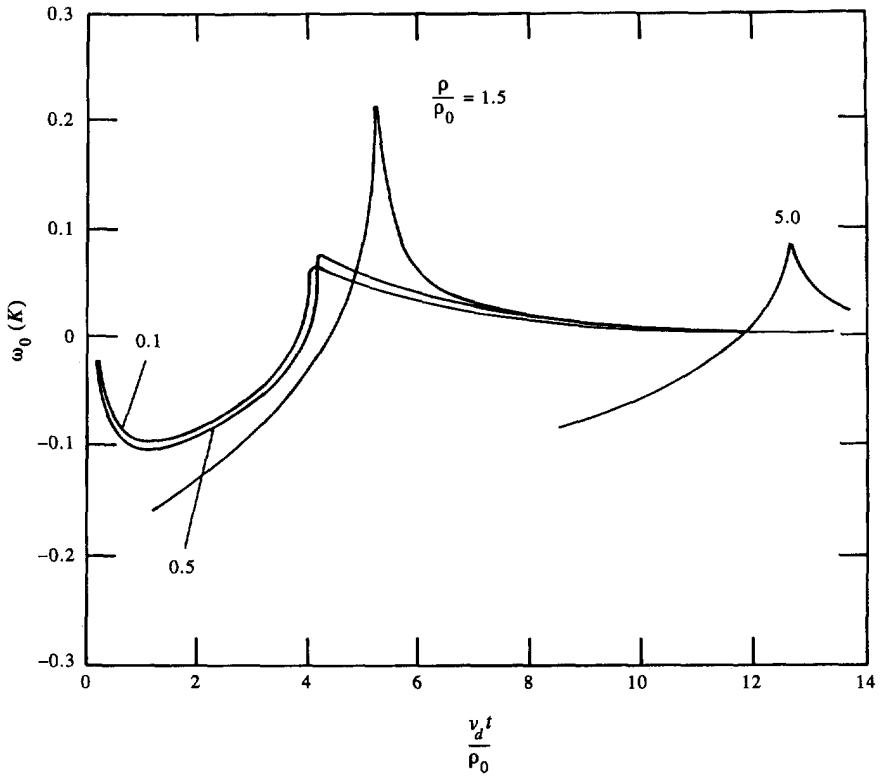

Fig. 3. Surface temperature change ω_o for uniform compressive surface stress.

and 4, respectively, vs the dimensionless time parameter $v_d t/\rho_o$ for various values of the dimensionless distance parameter ρ/ρ_o. The half-space is a steel with loading and material properties given by

$$\kappa = -7.1(10^{-5})\frac{1}{K}, \quad h = 8.2(10^{-4})\ \mu\text{m}, \quad \frac{\sigma_o}{\mu} = -0.01 \tag{64}$$

and Table 1. The mild requirements that $(v_d t/h, \rho_o/h) \gg 1$ should guarantee that the long-time restriction is met. The magnitude of the loading given by (64) is roughly one-half of the simple-tension test value for yield. The sign produces a compressive stress for the uniform loading case. The peaks seen in both Figs 3 and 4 for $\rho < \rho_o$ occur near $t = 2b_o\rho_o$, i.e., twice the travel time of a Rayleigh signal from the loading disk center to the point of interest or the signal travel time between two points equidistant from the disk center and diametrically opposite. This phenomenon of distinctive solution behavior at Rayleigh signal travel times is similar to that noted at the outset for dynamic fracture analysis.

It is also noted that the uniform loading case (Fig. 3) produces much smaller changes in surface temperature than those found for the zero-force case (Fig. 4), but that a strong decay with distance ρ from the disk center occurs for the latter. Another noticeable difference is that ω_o dies out rapidly with time in Fig. 3, while $|\omega_o|$ in Fig. 4 achieves steady-state values that vary inversely with distance. The maximum temperature change values—which occur in Fig. 4—are not critical, but are not negligible, either. Because no heat flux has been imposed on the surface in these examples, such values show that Rayleigh signal-induced changes in surface temperature can be an important effect.

SOME REMARKS

This article considered Rayleigh (surface) and Stoneley (interface) signals in transient 3D analyses of fully-coupled thermoelastic half-spaces under both mechanical and thermal loading. The first task in the study was to obtain exact expressions for the zeroes of the

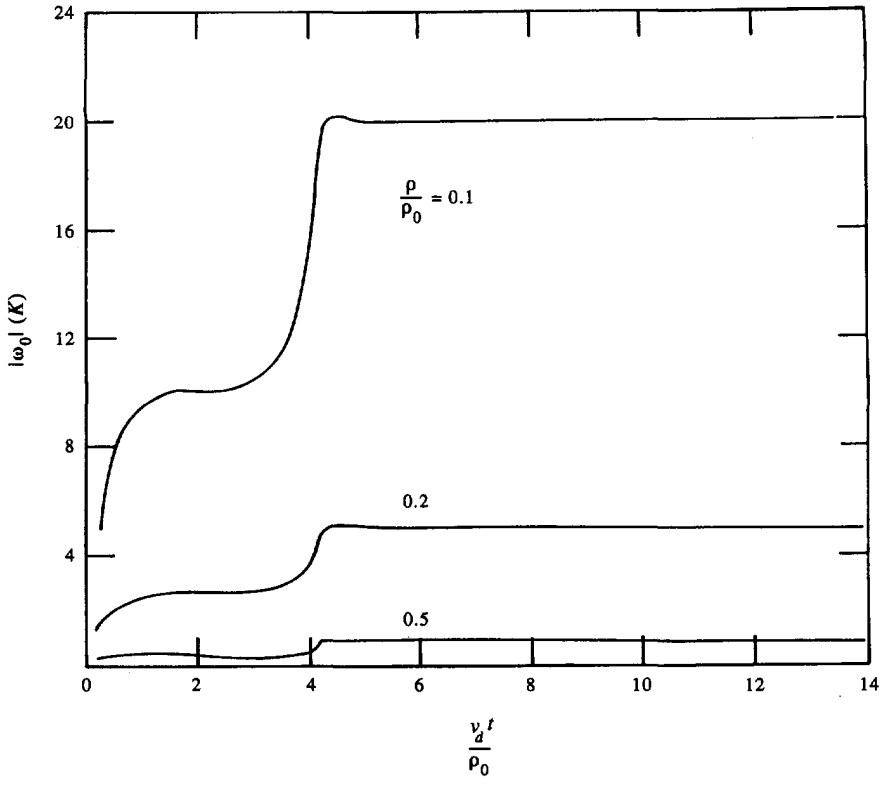

Fig. 4. Surface temperature change amplitude $|\omega_0|$ for zero-force surface stress.

Rayleigh/Stoneley functions that arise in the integral transforms of the corresponding problem solutions. These zeroes could be viewed as occurring in complex plane whose points are defined by a scalar resultant of two spatial transform variables, and the zeroes themselves depended on the temporal transform variable. Then, as illustrations of signal effects, the surface temperature changes associated with the Rayleigh signals generated by two types of normal stress surface loading were obtained by inverting for long times integral transform expressions that were valid near the Rayleigh zero locations.

The so-called long-time solution forms involved Rayleigh function zeroes that reduce to constants and, therefore, represent the inverses of classical Rayleigh wave speeds whose values are modified by thermal coupling. This behavior is consistent with that predicted by 2D results for a low-frequency time-harmonic form for a thermoelastic Rayleigh signal. For completeness, the corresponding long-time Stoneley signal zeroes were also given, and found to be thermally-modified inverses of classical Stoneley wave speeds. Despite such simplicity, the long-time results were robust, because time was scaled by a small thermoelastic characteristic length.

Calculations showed that, depending on the loading form, the Rayleigh signal can induce surface temperature changes that, instead of decaying with time, reach steady-state values. Moreover, the values achieved were not negligible, e.g., $O(10)$ K. Because no heat was imposed as part of the loading, these illustrations indicate that Rayleigh/Stoneley signals may well produce effects that are important in characterizing transient thermoelastic surface response.

This basic study did not address the related problem of pseudo-Rayleigh signals, e.g., (Brock, 1978), nor the question of precisely what types of thermal surface/interface conditions imposed will in fact produce Rayleigh/interface signals. However, as with the corresponding 2D results (Brock, 1995), it is hoped that this study will allow insight into transient surface/interface signal effects in thermoelastic materials. In particular, these results were obtained by treating complete problems of prescribed mechanical and thermal loadings, and the key Rayleigh/Stoneley function product-splitting operations would arise

in the solution of mixed boundary value problems by a Wiener-Hopf technique (Achenbach, 1973; Freund, 1990; Noble, 1958).

Acknowledgements—This work was supported by NSF Grant DMS 9121700 and by the NSF/EPSCoR Group in Inverse Problems and QNDE at the University of Kentucky.

REFERENCES

Abramowitz, M. and Stegun, I. A. (1972) *Handbook of Mathematical Functions*, Dover, New York.
Achenbach, J. D. (1973) *Wave Propagation in Elastic Solids*, North-Holland/American Elsevier, Amsterdam.
Brock, L. M. (1978) The effect of a thin layer surface inhomogeneity on dynamic surface response. *ASME Journal of Applied Mechanics* **45,** 95–99.
Brock, L. M. (1980) Wave propagation in an elastic half-space due to surface pressure over a non-uniformly changing circular zone. *Quarterly Applied Mathematics* **38,** 37–49.
Brock, L. M. (1981) The effects of displacement discontinuity derivatives on wave propagation—I. three-dimensional elastic solids. *International Journal of Engineering Science* **19,** 243–252.
Brock, L. M. (1982a) Shear and normal impact loadings on one face of a narrow slit. *International Journal of Solids and Structures* **18,** 467–477.
Brock, L. M. (1982b) The effects of displacement discontinuity derivatives on wave propagation—IV. Dislocation motion in a half-space. *International Journal of Engineering Science* **20,** 483–496.
Brock, L. M. (1992) Transient thermal effects in edge dislocation generation near a crack edge. *International Journal of Solids and Structures* **29,** 2217–2234.
Brock, L. M. (1993) Early effects of temperature-dependent yield-stress in a transient analysis of fracture. *Acta Mechanica* **97,** 101–114.
Brock, L. M. (1995) Some transient results for Rayleigh and Stoneley signals in thermoelastic solids. College of Engineering Technical Report, University of Kentucky, 1995.
Cagniard, L. (1962) *Reflection and Refraction of Progressive Seismic Waves* (E. A. Flinn and C. H. Dix, translators), McGraw-Hill, New York.
Chadwick, P. (1960) Thermoelasticity: the dynamical theory. In *Progress in Solid Mechanics*, Vol. 1 (eds I. N. Sneddon and R. Hill), pp. 265–330, North-Holland, Amsterdam.
Freund, L. B. (1974) The stress intensity factor due to normal impact loading on the faces of a crack. *International Journal of Engineering Science* **12,** 179–190.
Freund, L. B. (1990) *Dynamic Fracture Mechanics*, Cambridge University Press.
Gradshteyn, I. S. and Ryzhik, I. M. (1975) *Table of Integrals, Series and Products*, Academic Press, New York.
Hille, E. (1959) *Analytic Function Theory*, Vol. I, Ginn, Waltham, MA.
Lamb, H. (1904) On the propagation of tremors over the surface of an elastic solid. *Philosophical Transactions of the Royal Society* (London) **A204,** 1–12.
Liu, C., Huang, Y. and Rosakis, A. (1995) Shear dominated transonic interfacial crack growth in a bimaterial—II. asymptotic fields and favorable velocity regimes. *Journal of the Mechanics and Physics of Solids* **43,** 189–206.
Miklowitz, J. (1978) *The Theory of Elastic Waves and Waveguides*, North-Holland, Amsterdam.
Noble, B. (1978) *Methods Based on the Wiener-Hopf Technique*, Pergamon, New York.
Norwood, F. R. (1977) Response of an acoustic-elastic system to a transient source in the acoustic medium: analytical modeling for the air-coupled wave. *International Journal of Engineering Science* **15,** 391–404.
Nowinski, J. L. (1978) *Theory of Thermoelasticity with Applications*, Sijthoff and Noordhoff, Alphen aan Rijn.
Sneddon, I. N. (1972) *The Use of Integral Transforms*, McGraw-Hill, New York.
Stoneley, R. (1924) Elastic waves at the surface of separation of two solids. *Proceedings of the Royal Society* (London) **106,** 416–428.
van der Pol, B. and Bremmer, H. (1950) *Operational Calculus Based on the Two-Sided Integral*, Cambridge University Press.
Watson, G. N. (1966) *Theory of Bessel Functions*, Cambridge University Press.